Exciton sizes of conducting polymers predicted by time-dependent density functional theory

Sergei Tretiak*
Theoretical Division and Center for Nonlinear Studies, Los Alamos National Laboratory, Los Alamos, New Mexico 87545, USA

Kirill Igumenshchev
Department of Chemistry, University of Rochester, Rochester, New York 14627, USA

Vladimir Chernyak
Department of Chemistry, Wayne State University, Detroit, Michigan 48202, USA
(Received 24 September 2004; published 12 January 2005)

The electronic structure and size scaling of spectroscopic observables in conjugated polymers are investigated using time-dependent density functional theory. We show that local density approximations and gradient-corrected functionals do not have an effective attractive Coulomb interaction between photoexcited electron-hole pairs to form bound states and therefore do not reproduce finite exciton sizes. Long-range nonlocal and nonadiabatic density functional corrections (such as hybrid mixing with an exact Hartree-Fock exchange) are necessary to capture correct delocalization of photoexcitations in one-dimensional polymeric chains.

DOI: 10.1103/PhysRevB.71.033201 PACS number(s): 78.66.Qn, 78.55.Kz

An ability to model complex behavior of organic matter on the nanometer length scale is necessary for our understanding of fundamental electronic processes and designing new functional materials and devices. This frequently requires inclusion of electronic correlations and coupling of electrons to molecular structure. Time-dependent density functional theory (TD-DFT) recently became an effective tool for calculation of electronic excitations in both finite molecular systems and solids.[1,2] Being an extension of static DFT, TD-DFT is based on mapping of a time-dependent interacting system to a noninteracting Kohn-Sham (KS) system with the same density driven by an external perturbation.[1–3] In principle, TD-DFT is exact upon knowledge of the underlying functionals. Systematic development of functionals has been conducted for ground state properties and resulted in a significant improvement of static DFT performance.[4] However, sophisticated functionals do not necessary improve electronic spectra of molecules and solids, and strategies for systematic improvement of TD-DFT are yet to be developed.

TD-DFT accounts for many-body effects in the time-dependent exchange-correlation (xc) potential v_{xc} and its functional derivative f_{xc}.[1–3] Understanding and deriving f_{xc} are central goals in the improvement of TD-DFT. The frequently employed adiabatic approximation, which neglects memory effects in the density, does not always produces accurate results.[5] For example, in solids it fails to capture excitonic effects.[6] Recent studies explored the connection of TD-DFT to Görling-Levy perturbation theory,[7,8] the GW approximation[6,7] (GWA), and the Bethe-Salpeter equation (BSE).[9–11] The latter, for example, showed that inclusion of a long-range tail ($\sim 1/q^2$) to f_{xc} is necessary for reproducing of optical spectra in solids. The frequency dependence of the f_{xc} kernel[12,13] is also necessary for reproducing double excitations in finite molecules.[14] Many theoretical studies using first-principles computations such as TD-DFT are currently focused on conjugated polymers, which are important materials for a number of optoelectronic and photonic applications.[15,16] The complex electronic structure of these molecular systems reflects an interplay between many-body correlations and electron-phonon coupling.[16–18] Most of the previous studies of excited state structure in conjugated polymers with DFT methods utilized periodic boundary condition and the adiabatic local density approximation (ALDA) coupled with correlated GWA and BSE approaches.[19–21] Studies of finite size oligomers have been reported as well (e.g., Ref. 22). For example, the exciton binding energy was found to be strongly affected by intermolecular interactions[20,21] compared to the isolated chains.[19] The recent nonlocal density current Vignale-Kohn functional[23] has shown great promise by reproducing size scaling of static polarizablities in several conjugated chains.[24]

In this Brief Report we explore the applicability of different models of density functionals for resonant optical properties of one-dimensional conjugated polymers ranging from the small oligomers in the regime of quantum confinement all the way to the infinite chain length limit. We focus on how well various DFT functionals reproduce the correct scaling of spectroscopic observables with the system size and investigate appearing failures of the ALDA and gradient-corrected models. We start with computations of electronic excitations in the oligomers of various lengths ($N=2$–20) of poly (*p*-phenylene vinylene) (PPV) shown in the inset of Fig. 1 using the Gaussian 98 suite.[25] The results of this study will be similar for any other one-dimensional polymeric chain featuring delocalized π-electronic system, irrespective of particular chemical composition.[15] A 6-31G basis set was used for all calculations. Molecular geometries have been optimized using the Hartree-Fock (HF) approach, which we previously found[26] to be is superior to the DFT approach by reproducing accurately the bond length alternation parameter in similar conjugated systems when compared to experiment. Next we calculated up to 20 singlet electronic states for each molecule using TD-DFT coupled with different functionals. We employed most commonly used functionals such as ALDA, gradient-corrected functionals [Perdew, Burke, and Ernzerhof functional (PBE) and Becke, Lee, Yang, and Parr functional (BLYP)], and hybrid functionals [Becke 3-parameter hybrid functional (B3LYP), hybrid Perdew,

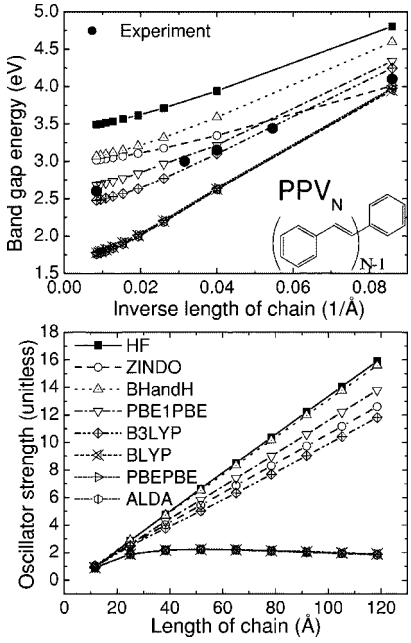

FIG. 1. Scaling and saturation of calculated and experimental (Ref. 22) band-gap ($1B_u$ state) energies (top panel) and the respective oscillator strengths with the PPV oligomer size. The inset shows the structure of PPV.

Burke, and Ernzerhof functional (PBE1PBE), and hybrid half-and-half functional (BHandH), which contain 20%, 25%, and 50% of HF exchange, respectively]. Calculations using the TD-HF approach coupled with *ab initio* and semiempirical INDO/S Hamiltonians were conducted as well to explore the limiting case with 100% of HF exchange.

The results for the lowest singlet excited state ($1B_u$) of PPV, which plays a major role in absorption, photoluminescence, and carrier transport, are shown in Fig. 1. As expected,[27] calculated band gap frequencies exhibit nearly linear scaling with the inverse chain length saturating to the constants in a long chain limit for all methods (top panel). ALDA and gradient corrected functionals produce very similar results. Hybrid functionals result in a consistent blueshift of the transition energy depending on the amount of HF exchange present in the functional. Overall B3LYP results for both small ($N=2$) molecule (4.2 eV) and infinite polymer (2.4 eV) are in the best agreement with experiment (4.1 and 2.5 eV, respectively) whereas pure DFT functionals consistently underestimate the band gaps. The bottom panel of Fig. 1 displays variation of the corresponding oscillator strengths f as a function of chain length. Only HF and hybrid functionals produce the correct linear scaling of f with the chain length. Oscillator strengths calculated with ALDA and gradient-corrected functionals exhibit drastically different scaling properties that are inconsistent with simple physical reasoning and experimental observations.

To rationalize these trends we further use two-dimensional real-space analysis of transition densities $(\xi_\nu)_{mn}$, representing the electronic transitions between the ground state and electronically excited states.[27] In the TD-HF approach, the diagonal elements of these quantities $(\xi_\nu)_{nn}$ represent the net charge induced in the nth atom by an external

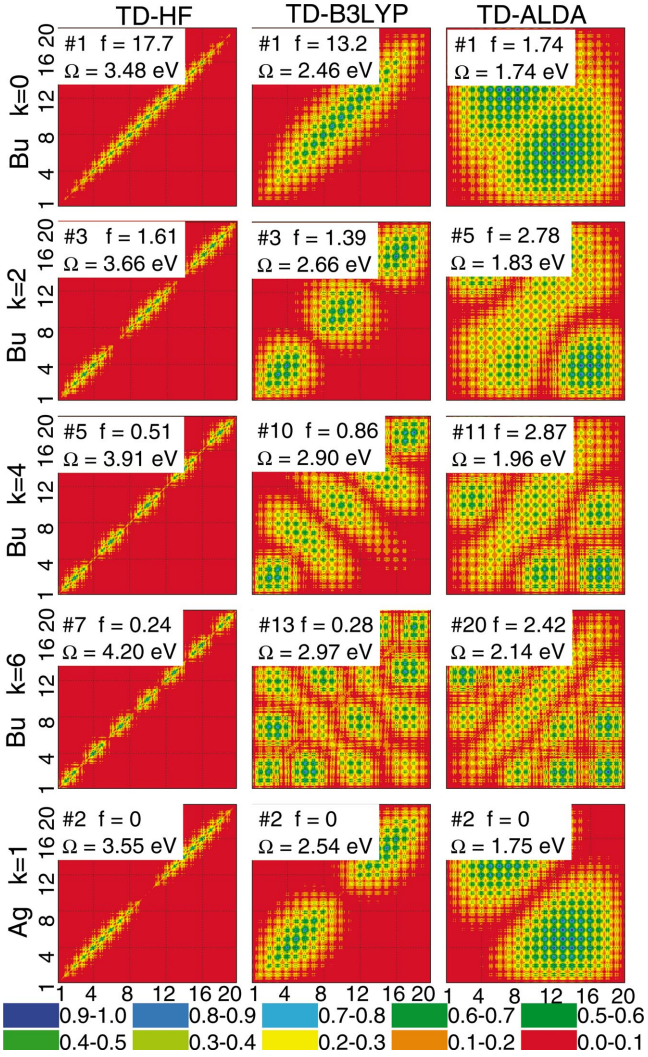

FIG. 2. (Color) Contour plots of transition density matrices from the ground state to low-energy excited states in PPV_{20}. The insets give corresponding state number, oscillator strength, and transition frequency. The axis labels represent individual repeat units along the oligomer chain. The color code is given at the bottom. Each plot depicts probabilities of an electron moving from one molecular position (horizontal axis) to another (vertical axis) upon electronic excitation.

field. The off-diagonal elements $(\xi_\nu)_{mn}$ with $m \neq n$ represent the joint probability amplitude of finding an electron and a hole located at the mth and nth atoms, respectively.[27] Thus, the transition densities make it possible to interpret electronic transitions with optically induced charges and electronic coherences. A very similar interpretation can be applied to the transition densities obtained with TD-DFT approaches.

The left column of Fig. 2 displays contour plots of the transition densities corresponding to several low-lying excited states in PPV_{20} calculated using *ab initio* TD-HF method. The band gap transition (1) has the largest oscillator strength and is very similar to that calculated with semiempirical Hamiltonians.[27] This picture shows that the electron-hole pair created upon optical excitation is delocalized over the entire chain (diagonal in the plot). The exciton

size is about 2 repeat units (largest off-diagonal extent of the nonzero matrix area). Higher-lying electronic transitions have an increasing number of diagonal nodes (e.g., no. 3 is broken into the three parts).[28] These states can be interpreted as transitions with nonzero angular momenta in the limit of the infinite chain length.[28,29] The right column of Fig. 2 displays transition densities calculated using the TD-ALDA method. These are dramatically different from the TD-HF densities. It is immediately obvious that the band-gap transition 1 does not correspond to the *bound exciton* state. An electron tends to stay in the first half when a hole is in the second half of the chain (or *vice versa*). This indicates an effective *repulsive* Coulomb interaction between an electron and a hole. The diagonal elements are small and, therefore, the oscillator strength of this transition is low. Higher-lying electronic transitions are also completely delocalized having similar well-separated electron-hole pairs and weak oscillator strengths. The energetic spacing between electronic states is reduced compared to that in the TD-HF method. Thus ALDA and gradient corrected functionals (not shown) result in a band of quasidegenerate states corresponding to *unbound excitons* with the oscillator strength of the band gap dispersed among many states. This explains the anomalous scaling behavior of the band-gap oscillator strength in Fig. 1. In contrast, all hybrid functionals that mix the HF exchange with ALDA and gradient corrections have a bound exciton state. The middle column of Fig. 2 shows results obtained with the TD-B3LYP method (20% of HF exchange). The structure of TD-B3LYP transition densities is very similar to the structure of TD-HF densities. However, the exciton size is larger and grows for higher electronic states. The electron-hole interaction can be interpreted as a competition between a long-range Coulomb attraction induced by HF exchange and local strong repulsion brought by the ALDA component. The size of the exciton and, therefore, an effective Coulomb attraction between an electron and a hole depend on the amount of the HF exchange in the functional.

Figure 3 emphasizes this attraction-repulsion interplay by showing variations of the band-gap energy and the highest occupied-lowest unoccupied molecular orbitals gap (HOMO-LUMO) for small and large chains as a function of the Hamiltonian model. The band-gap energy is smaller than the HOMO-LUMO gap for both molecules in the HF method because an effective electron-hole attraction stabilizes the HOMO-LUMO gap (which corresponds to noninteracting particles). In contrast, the situation is opposite in ALDA and gradient-corrected models in the small ($N=2$) molecule due to electron-hole repulsion. In the large ($N=20$) chain, when an electron and a hole can be well separated and their localized repulsion is no longer relevant, the band gap asymptotically coincides with the HOMO-LUMO gap (a typical property of TD-DFT in solids[10,11]).

Thus pure TD-ALDA and TD-HF methods roughly represent two extreme cases of Wannier-Mott and Frenkel excitons, repectively. Previous theoretical and experimental studies have unambiguously shown that conjugated polymers belong to an intermediate class, which can be described by hybrid functionals spaning all ranges between HF and ALDA extremes. For example, the exciton size in PPV is about 6–7 (B3LYP), 5–6 (PBE1PBE), 3–4 (BHandH) repeat units in

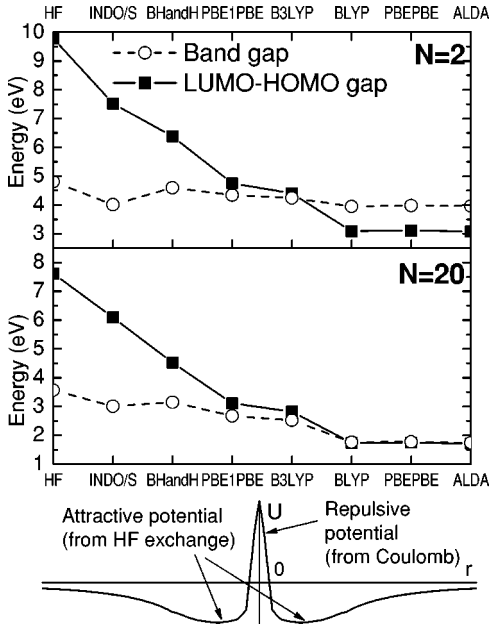

FIG. 3. Variation of HOMO-LUMO gap and band gap energies as a function of Hamiltonian model in short, PPV_2 (top panel) and long, PPV_{20} (middle panel) oligomers, which mimic confined and infinite chain limits, respectively. The bottom panel schematically shows an effective potential between an electron and a hole in the hybrid TD-DFT case.

TD-DFT approaches compared to 4–5 repeat units in the INDO/S semiempirical model,[17,27] 5–6 (Ref. 30) and 4–5 (Ref. 31) repeat units in correlated GWA and BSE ab *initio* approaches, and 5–7 repeat units in experiment[32–34] (given the uncertainty of conformational disorder and interchain interactions).

To rationalize these numerical results we consider a model density functional based on the Pariser-Parr-Pople Hamiltonian for an infinite one-dimensional π-conjugated (polyene) chain, where each carbon atom n has a single π orbital with the nearest-neighbor hopping $t_{2n,2n\pm1}=(1\pm\zeta/2)t_0$ (ζ being Peierls distortion parameter).[27] On the level of adiabatic TD-DFT, the system can be described as classical dynamics in the phase space of KS single-electron density matrices ρ_{mn} with the KS Hamiltonian

$$H(\rho)=\sum_n\left(t_{n,n+1}\rho_{n+1,n}+\frac{1}{2}\sum_{mn}U_{m-n}\rho_{mm}\rho_{nn}+c_x\frac{1}{2}\sum_{mn}U_{m-n}\rho_{mn}\rho_{nm}+E_{xc}(\rho_{nn})\right), \quad (1)$$

where U_{m-n} stands for the Coulomb potential and E_{xc} is a local functional (if the orbital overlap is neglected). The hybrid mixing parameter $c_x\leqslant 1$ (Ref. 4) accounts for the amount of HF exchange. Since the symmetry breaking, the ground state is represented by the bond-length alternation wave with $\bar{\rho}_{nn}=0.5$ for all n. This implies that the ground-state Coulomb and exchange-correlation potentials are homogeneous, and the KS orbitals are determined by the hopping term solely. In the momentum representation and the

basis set of molecular orbitals (characterized by their momenta $-\pi \leqslant s \leqslant \pi$ with respect to the discrete translation over a unit cell), the linear response is given by the deviations $\xi_{ss'}$ of the particle-hole components of the KS density matrix from its ground state.[29] Since the total momentum of the electron-hole pair is a well-defined quantum number, the modes with zero momentum contributing the optical response can be described by the functions $\bar{f}_{\pm}(s)$ ($\bar{f}_{+}$ and $\bar{f}_{-}$ being particle-hole and hole-particle components, respectively). Since typically $|\bar{f}_{-}| \ll |\bar{f}_{+}|$, we set $\bar{f}_{-}(s)=0$ for a qualitative analysis.

The hybrid density functional case [Eq. (1)] can be considered within the framework of Ref. 29 by weighting the exchange terms with c_x and using the renormalized potential $U^r_{m-n}=U_{m-n}+\delta_{mn}f_{xc}(\bar{\rho}_{nn}=0.5)$ ($f_{xc}=v'_{xc}=E''_{xc}$) to include the effects of correlations. We can then recast the TD-HF eigenmode equation [Eq. (D9) in Ref. 29] for TD-DFT case in a form

$$[\epsilon(s)-\Omega]\bar{f}_{+}(s)+c_x\int\frac{ds'}{2\pi}\bar{V}^{(0)}(s-s')\bar{f}_{+}(s') + \bar{V}^{(r)}(0)\int\frac{ds'}{2\pi}\bar{f}_{+}(s')=0, \tag{2}$$

with $\epsilon(s)=2t_0[\zeta^2+2(1-\zeta^2)(1+\cos s)]^{1/2}$, Ω is an excitation frequency, and $\bar{V}^{(0)}(s-s')$ is an effective Coulomb potential [Eq. (D10) in Ref. 29]. The presence of HF exchange is accounted for by two numbers: The coefficient c_x and the renormalized quantity $\bar{V}^{(r)}(0)>0$ **(**instead of $\bar{V}^{(1)}(0)>0$ [Eq. (D10) in Ref. 29] used in the pure TD-HF case**)**. Using an effective mass approximation and switching back to the coordinate representation, Eq. (2) can be interpreted as a one-dimensional Schrödinger equation where the $c_x\bar{V}^{(0)}$ term represents a long-range binding potential, whereas the $\bar{V}^{(r)}(0)$ term stands for a local repulsive contact potential (see bottom panel in Fig. 3). This implies that without HF hybrid mixing a bound state cannot be formed in an infinite system, and the optical gap is given by the HOMO-LUMO gap. Note that $\bar{V}^{(1)}(0)>0$ reflects the repulsive nature of the electron-electron Coulomb interaction, whereas the binding property of $\bar{V}^{(0)}$ in Eq. (2) is inherited from the attractive nature of the Fock exchange (i.e., the Coulomb attractive electron-hole interaction).

In conclusion, we have studied performance of the TD-DFT approach and modern density functionals for electronic excitations in conjugated polymers. ALDA and gradient-corrected functionals result in unphysical unbound exciton states due to an effective Coulomb repulsive interaction. Correlated methods such as GWA and BSE (which may be built on the top of ALDA) overcome this problem[6,7,9–11] but can be practically applied only to infinite-dimensional systems when periodic boundary conditions are imposed. Hybrid functionals circumvent this problem as well by mixing the exact HF exchange, which effectively is an extension to nonadiabatic TD-DFT. The latter follows from the fact that the Fock exchange terms, being adiabatic in terms of the KS density matrix, can be recast as a nonadiabatic functional of the electron density alone. An appropriate amount of the exact HF exchange can be further fine-tuned by fitting to the size scaling of experimental spectroscopic observables. Thus hybrid functionals represent a practical and accurate way for the correct description of excited states at all molecular length scales from small clusters to bulk materials.

The authors thank R.L. Martin and R. Magyar for their critical comments. The research at LANL is supported by Center for Nonlinear Studies (CNLS) the LDRD program of the US Department of Energy. This support is gratefully acknowledged.

*Electronic address: serg@cnls.lanl.gov

[1] E. K. U. Gross *et al.*, *Density Functional Theory II* (Springer, Heidelberg, 1996), Vol. 181, p. 81.
[2] M. E. Casida, in *Recent Advances in Density-Functional Methods, Part I*, edited by D. A. Chong (World Scientific, Singapore, 1995), Vol. 3.
[3] E. Runge and E. K. U. Gross, Phys. Rev. Lett. **52**, 997 (1984).
[4] E. K. U. Gross *et al.*, and M. Petersilka, in *Density Functional Theory*, edited by R. F. Nalewajski (Springer, Berlin, 1996), Vol. 181.
[5] Z.-L. Cai *et al.*, J. Chem. Phys. **117**, 5543 (2002).
[6] G. Onida *et al.*, Rev. Mod. Phys. **74**, 601 (2002).
[7] X. Gonze and M. Scheffler, Phys. Rev. Lett. **82**, 4416 (1999).
[8] H. Appel *et al.*, Phys. Rev. Lett. **90**, 043005 (2003).
[9] P. Ghosez *et al.*, Phys. Rev. B **56**, 12811 (1997).
[10] L. Reining *et al.*, Phys. Rev. Lett. **88**, 066404 (2002).
[11] F. Sottile *et al.*, Phys. Rev. Lett. **91**, 056402 (2003).
[12] I. V. Tokatly and O. Pankratov, Phys. Rev. Lett. **86**, 2078 (2001).
[13] V. Chernyak and S. Mukamel, J. Chem. Phys. **112**, 3572 (2000).
[14] N. T. Maitra *et al.*, Phys. Rev. Lett. **89**, 023002 (2002).
[15] A. J. Heeger, Rev. Mod. Phys. **73**, 681 (2001).
[16] A. J. Heeger *et al.*, Rev. Mod. Phys. **60**, 781 (1988).
[17] J. L. Brédas *et al.*, Acc. Chem. Res. **32**, 267 (1999).
[18] S. Tretiak *et al.*, Phys. Rev. Lett. **89**, 097402 (2002).
[19] M. Rohlfing and S. G. Louie, Phys. Rev. Lett. **82**, 1959 (1999).
[20] A. Ruini *et al.*, Phys. Rev. Lett. **88**, 206403 (2002).
[21] J. W. van der Horst *et al.*, Phys. Rev. Lett. **83**, 4413 (1999).
[22] A. Pogantsch *et al.*, J. Chem. Phys. **117**, 5921 (2002).
[23] G. Vignale and W. Kohn, Phys. Rev. Lett. **77**, 2037 (1996).
[24] M. van Faassen *et al.*, Phys. Rev. Lett. **88**, 186401 (2002).
[25] M. J. Frisch *et al.*, *Gaussian 98 (Revision A.11)* (Gaussian, Inc., Pittsburgh, PA, 2002).
[26] A. M. Masunov and S. Tretiak, J. Phys. Chem. B **108**, 899 (2004).
[27] S. Tretiak and S. Mukamel, Chem. Rev. (Washington, D.C.) **102**, 3171 (2002).
[28] V. Chernyak *et al.*, Phys. Rev. Lett. **86**, 995 (2001).
[29] V. Chernyak *et al.*, J. Phys. Chem. A **105**, 1988 (2001).
[30] J. W. van der Horst *et al.*, Chem. Phys. Lett. **334**, 303 (2001).
[31] A. Ruini *et al.*, Synth. Met. **119**, 257 (2001).
[32] V. I. Arkhipov and H. Bassler, Phys. Status Solidi A **201**, 1152 (2004).
[33] A. Kohler *et al.*, Nature (London) **392**, 903 (1998).
[34] E. M. Conwell, Phys. Rev. Lett. **78**, 4301 (1997).